THE JOURNAL OF PHYSICAL CHEMISTRY B LETTERS

2005, *109,* 19556−19559
Published on Web 09/29/2005

Direct Evidence for Root Growth of Vertically Aligned Single-Walled Carbon Nanotubes by Microwave Plasma Chemical Vapor Deposition

Takayuki Iwasaki, Goufang Zhong, Takumi Aikawa, Tsuyoshi Yoshida, and Hiroshi Kawarada*

Department of Science and Engineering, Waseda University, 3-4-1 Ohkubo, Shinjuku-ku, Tokyo

Received: August 10, 2005; In Final Form: September 19, 2005

The root growth mode of extremely dense and vertically aligned single-walled carbon nanotubes (SWNTs) synthesized by microwave plasma chemical vapor deposition was clarified by a new method, marker growth, which does not require transmission electron microscopy. SWNT layers were grown intermittently on a substrate, and a line between the layers was used as a marker to identify the growth mode. Micro-Raman spectroscopy revealed that the SWNT layers have the same diameter distribution.

It is essential to control the growth direction of SWNTs on a substrate for fabrication of SWNT-based applications, such as field effect transistors (FETs)[1−4] and interconnects for ULSI.[5] Chemical vapor deposition (CVD) is a reliable method for the controlled growth of SWNTs as an alternative to arc discharge[6] and laser ablation.[7] Recent progress has made it possible to directly grow vertically aligned SWNTs by both thermal- and plasma-assisted CVD.[8−12] Using a point-arc microwave plasma (PA-MP) CVD apparatus, we have achieved very high yield, selective growth of vertically aligned SWNTs on Si substrates coated with a sandwich-like structure of Al_2O_3/Fe/Al_2O_3(/Si).[10,11] For further control of growth, it is important to investigate the growth mode of SWNTs. Multiwalled carbon nanotubes (MWNTs) can grow by either the root growth mode or the tip growth mode according to the residing positions of catalytic nanoparticles, which can be observed easily by scanning electron microscopy (SEM).[13−16] However, in the case of SWNTs, catalytic particles can hardly be observed by SEM because of their small size. Even if a catalytic particle attached to the SWNT[17,18] or a closed SWNT with no catalyst at the tip[12] can be observed by transmission electron microscopy (TEM), it is difficult to evaluate the growth mode of SWNTs in macroscopic quantities. In the present study, a novel experimental method called marker growth was used to determine the growth mode of a number of as-grown vertically aligned SWNTs by PA-MP CVD.

Hata et al.[9] reported that their vertically aligned SWNTs prepared by thermal CVD showed root growth by removing aligned SWNTs from the substrate using a razor blade and synthesizing SWNTs again on the same substrate. However, it is possible that unreacted catalytic particles at first growth nucleate and synthesize new SWNTs at regrowth. Moreover, hand cutting using a razor blade has poor reproducibility.

To confirm the growth mode of vertically aligned SWNTs, we designed a new method, marker growth. Switching off the plasma after growth of MWNTs allows them to continue growing under thermal CVD conditions using C_2H_2 and NH_3 gases at a high temperature of 825 °C.[19] The MWNTs grown in thermal CVD have a different appearance from those grown in plasma CVD; MWNTs grown in plasma CVD are straight and aligned vertically, while thermal CVD conditions result in random or curly MWNTs. We expected a similar phenomenon for our SWNTs. If we stop the plasma and heater after growth of SWNTs (the first layer, referred to as "1st" in Figure 1a,b), very short SWNTs could be formed using residual carbon precursors in the chamber, and the rapid decrease in temperature could cause defects in the SWNTs. When the plasma and heater are turned on again, SWNTs grow again on the same substrate (the second layer, referred to as "2nd" in Figure 1c,d). Our SWNTs grow at a constant growth rate in a few hours, and the top surface is very flat. Therefore, by changing the growth time for the second layer (shorter time case shown in Figure 1), we could identify the first and second layers using the part grown by the residual carbon precursors as a marker and determine the growth mode of vertically aligned SWNTs.

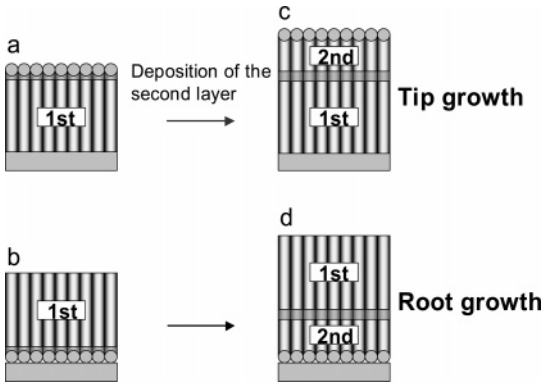

Figure 1. Model for determining the growth mode of vertically aligned SWNTs. (a, b) The first layer grown through the tip and the root growth mode, respectively. Short, dark gray part shows SWNTs grown by residual carbon precursors after switching off the plasma. (c, d) Deposition of the second layer in a shorter growth time than the first layer.

PA-MP CVD was used for the growth of vertically aligned and extremely dense SWNTs on Si wafers with a sandwich-

* kawarada@waseda.jp.

10.1021/jp054465t CCC: $30.25

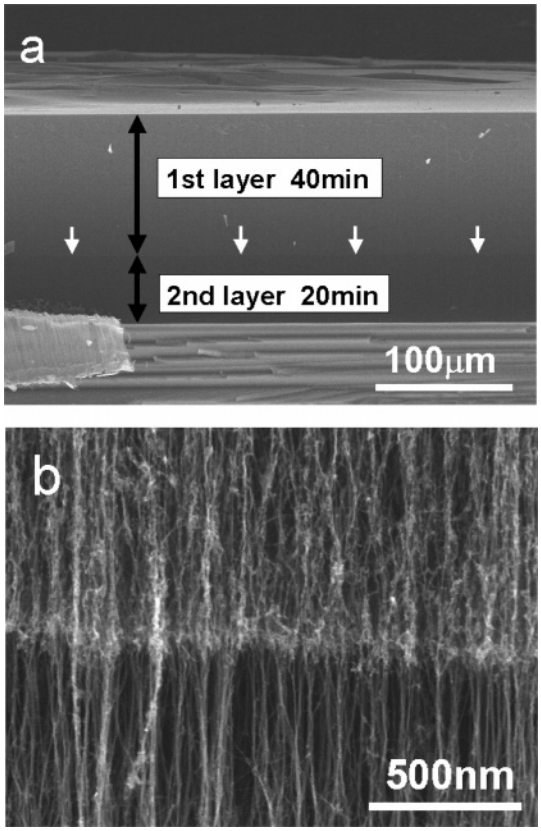

Figure 2. Cross-sectional SEM images of vertically aligned SWNTs grown intermittently. (a) A sample composed of two layers. White arrows indicate a marker. (b) Magnified image of the marker.

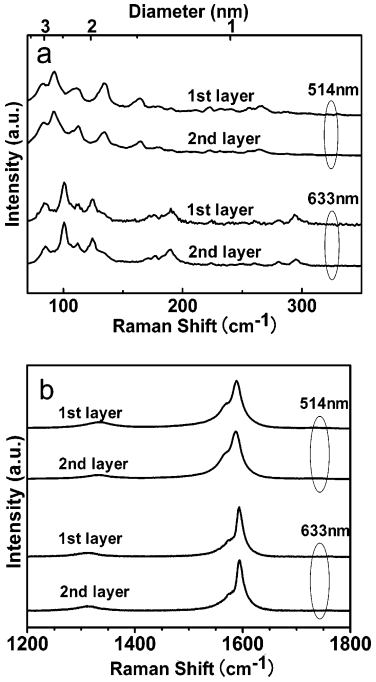

Figure 3. Raman spectra of the two SWNT layers grown intermittently, measured using 514 and 633 nm lasers. (a) Raman data for RBM of two layers. (b) Large-range Raman data including the G- and D-bands.

like structure of Al_2O_3 (0.5 nm)/Fe (0.3−0.5 nm)/Al_2O_3 (5 nm). The Al layer coated using a high-frequency magnetron sputtering on a Si wafer was oxidized in air to form an Al_2O_3 layer. Then, thin Fe and Al layers were coated on the Al_2O_3 layer. The top Al layer was also oxidized in air. The Fe film acts as a catalyst,

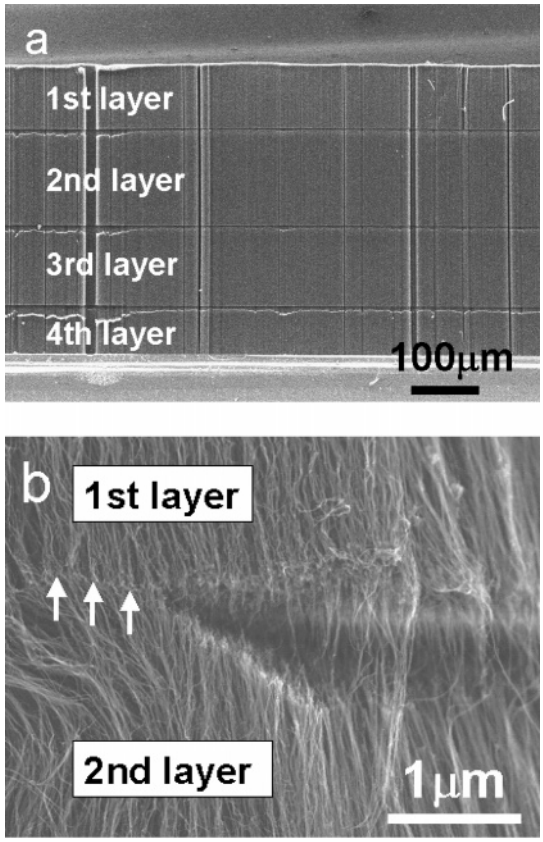

Figure 4. SEM image of peel-off at markers. (a) Four layers of SWNTs grown by marker growth. Three markers were confirmed between the layers, but peel-off of the layers was observed at all markers. (b) Magnified image of peel-off at a corner. White arrows show the uncut marker. The peeling was caused by cutting the substrate for the cross-sectional SEM observation.

and the Al_2O_3 layer beneath the Fe film acts as a buffer layer to prevent Si and Fe from reacting, while the Al_2O_3 layer above the Fe film increases the surface diffusion barrier of catalytic atoms markedly so that the aggregation of Fe atoms can be suppressed during the preheating period. As a result, a high density of small Fe particles is obtained, which is essential to synthesize the extremely dense and vertically aligned SWNTs.

Vertically aligned SWNTs were grown intermittently as follows. The substrate was heated at 600 °C for 5 min for preheating, and a microwave power of 60 W was applied in a mixture of H_2 and CH_4 gases (flow rates of H_2 and CH_4 were 45 and 5 sccm, respectively; total pressure = 20 Torr) in 40 min for growth of the first layer. Then, the plasma and heater were switched off, and the sample was cooled for 30 min, after which the substrate was heated at 600 °C and the plasma was turned on again for 20 min to allow the growth of the second layer. Then, the system was cooled.

Figure 2a shows a cross-sectional FE-SEM (Hitachi FE-SEM S-4800) image of a synthesized film in which a line can be seen marked with white arrows. This line is expected to be SWNTs grown from the residual carbon precursors and acts as a marker. We cannot exclude the possibility that the marker is simply a consequence of stopping the reaction, i.e., turning off the plasma. Figure 2b shows a higher magnification view of the marker. A different appearance was observed perpendicular to the orientation of SWNTs, but details of the structure are not yet clear. In comparison with the illustrations in Figure 1, the growth mode of vertically aligned SWNTs can be revealed

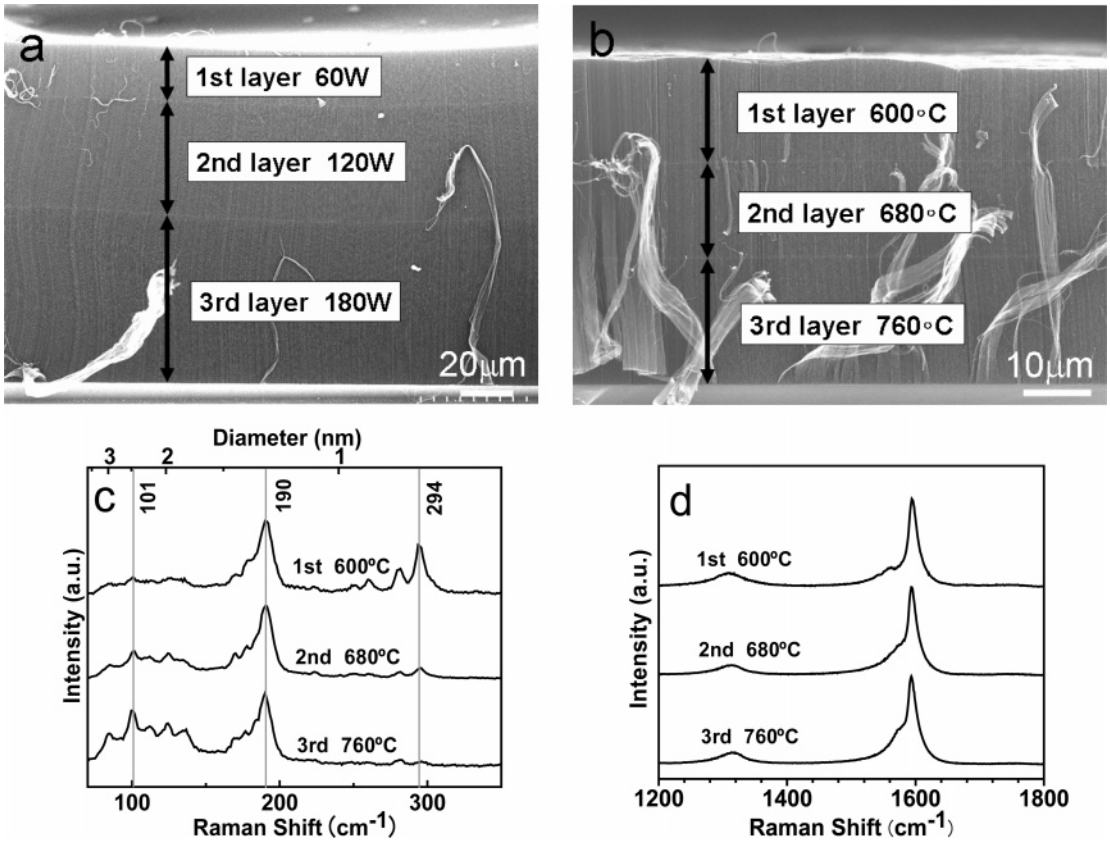

Figure 5. Marker growth performed under various CVD conditions. (a) SEM image of three layers grown at 60, 120, and 180 W. (b) SEM image of three layers grown at 600, 680, and 760 °C. (c) Raman data for RBM of (b), measured using a 633 nm laser. (d) Large-range Raman data of (b) including the G- and D-bands.

as root growth. The marker was formed in all SWNT samples and confirmed the root growth mode of a large number of SWNTs.

Characterization of the first and second layers was performed by micro-Raman spectroscopy (Renishaw inVia Raman microscope). Cross-sections of SWNT layers were also used for Raman measurements. We used two excitation lasers with wavelengths of 514 and 633 nm to evaluate the diameters of SWNTs over a wide range. Radial breathing mode (RBM) peaks of SWNTs can be seen clearly in Figure 3a. The diameter was estimated using the correlation, $d = 232/(\nu\text{-}6.5)$, where d is the diameter of SWNT in nanometers and ν is the Raman shift in reciprocal centimeters.[20] The first and second layers showed almost the same radial breathing mode peaks. No large shift was seen in the diameter distribution after deposition of the second layer. From this result, we inferred that SWNTs of the second layer grew using the same catalyst particles, the sizes of which were kept constant during growth of the first layer and the cooling period. Note that we performed measurements at the center of each layer, and the resolution of the lateral direction of the micro-Raman apparatus is a few micrometers with a 50× objective lens, so all of the Raman signal arose from each layer.

Figure 2b shows bundles of SWNTs of the first and second layers, but the structure of the marker is not clear. The marker growth can be performed many times, e.g., Figure 4a shows a sample composed of four layers grown by marker growth. When the substrate was cut for FE-SEM observation, the layers below the markers peeled off from those above the marker, indicating that SWNTs of the layers did not connect completely. We speculate that a layer below the marker connected weakly with the marker grown by residual carbon precursors after switching off the plasma because of defects caused by growth during the period of rapid temperature decrease.

The examination of marker growth is not limited to the set of conditions outlined above, and we performed experiments under various CVD conditions for deposition of each layer. Figure 5a shows three layers grown under different microwave powers: 60 W for the first layer, 120 W for the second, and 180 W for the third. Growth time was 5 min for all three layers, and other conditions were also the same. Normally, higher microwave power is associated with faster SWNT growth rate, because the amount of carbon precursors increases at higher microwave powers. Therefore, the growth mode of the sample in Figure 5a is root growth.

Moreover, growth temperature can also be changed for each layer deposition (Figure 5b). Raman spectra measured with an excitation wavelength of 633 nm showed different profiles (Figure 5c,d). High temperature should result in better crystallinity of SWNTs and a higher ratio of G to D peaks, indicating the root growth mode of the sample in Figure 5b. As the temperature increased, predominant peaks of RBM shifted to the lower-frequency region. SWNTs with larger diameters were synthesized at higher growth temperatures. Although the peaks at 294 cm^{-1} and 190 cm^{-1} were prominent at 600 °C, the peak at 294 cm^{-1} was decreased markedly at 680 °C and 760 °C. In contrast, the peak at 101 cm^{-1} increased at 680 °C and 760 °C. Maruyama et al.[21] also reported that high growth temperature resulted in synthesis of SWNTs with larger diameters using alcohol CVD. We speculate that catalytic particles were strongly anchored with the substrate and they became slightly flatter in shape under high temperatures. As a result, the diameter distribution of SWNTs shifted to the large region at the deposition of the second and third layers. The structure of

junctions between SWNTs with different diameters is an interesting issue and is now under investigation in our laboratory. Here, we confirmed that marker growth can occur under various CVD conditions. In addition, the PA-MP CVD apparatus used in this study has an antenna 50 mm from the substrate, and SWNTs are grown with carbon radicals generated at the antenna. Thus, the apparatus is similar to a thermal CVD system. We believe that marker growth can be performed under both plasma-enhanced and non-plasma-enhanced CVD conditions.

To clarify the growth mode of the dense and vertically aligned SWNTs, we proposed a new method, marker growth, which can be used to determine the growth mode of vertically aligned SWNTs without requiring complicated and time-consuming experiments. Therefore, this method can overcome the quantitative limitation of TEM observation. The root growth mode of a large quantity of vertically aligned SWNTs was determined successfully using a horizontal line between the two SWNT layers as a marker.

Although we have succeeded in synthesizing SWNTs with lengths on the order of millimeters, the growth rate of SWNTs decreases gradually as the length of SWNTs increases over 1 mm.[22] Carbon precursors are blocked to diffuse to catalytic particles on the substrate by a high density of long SWNTs. When SWNTs grow by the tip growth mode, carbon precursors can arrive at the catalysts at the tips of SWNTs without interruption of diffusion by SWNTs.[23] Tip growth is very attractive for the growth of long SWNTs, so it is better to show that marker growth works properly in the case of tip growth. However, unfortunately, we could not determine the conditions appropriate for tip growth of SWNTs in the present study. For MWNTs, different materials for the buffer layer lead to both tip and root growth modes.[15] Investigations using combinations of different catalysts and buffer layers and various CVD conditions are required for the tip growth of SWNTs. Our method is very useful to investigate the growth mode of dense and vertically aligned SWNTs.

Acknowledgment. This work is supported in part by a Grant-in-Aid for Center of Excellence (COE) Research from the Ministry of Education, Culture, Sports, Science, and Technology.

References and Notes

(1) Tans, S. J.; Verschueren, A. R. M.; Dekker, C. *Nature (London)* **1998**, *393*, 49−52.

(2) Wind, S. J.; Appenzeller, J.; Martel, R.; Derycke, V.; Avouris, P. *Appl. Phys. Lett.* **2002**, *80*, 3817−3819.

(3) Javey, A.; Wang, Q.; Ural, A.; Li, Y.; Dai, H. *Nano Lett.* **2002**, *2*, 929−932.

(4) Graham, A. P.; Duesberg, G. S.; Seidel, R.; Liebau, M.; Unger, E.; Kreupl, F.; Hönlein, W. *Diamond Relat. Mater.* **2004**, *13*, 1296−1300.

(5) Nihei, M.; Haribe, M.; Kawabata, A.; Awano, Y. *Jpn. J. Appl. Phys.* **2004**, *43*, 1856−1859.

(6) Journet, C.; Maser, W. K.; Bernier, P.; Loiseau, A.; Lamy de la Chapelle, M.; Lefrant, S.; Deniard, P.; Lee, R.; Fischer *Nature (London)* **1997**, *388*, 756−758.

(7) Thess, A.; Lee, R.; Nikolaev, P.; Dai, H.; Petit, P.; Robert, J.; Xu, C.; Lee, Y. H.; Kim, S. G.; Rinzler, A. G.; Colbert, D. T.; Scuseria, G. E.; Tomanek, D.; Fischer, J. E.; Smalley, R. E. *Science* **1996**, *273*, 483−487.

(8) Murakami, Y.; Chiashi, S.; Miyauchi, Y.; Minghui, H.; Ogura, M.; Okubo, T.; Maruyama, S. *Chem. Phys. Lett.* **2004**, *385*, 298−303.

(9) Hata, K.; Futaba, D. N.; Mizuno, K.; Namai, T.; Yumura, M.; Iijima, S. *Science* **2004**, *19*, 1362−1364.

(10) Zhong, G.; Iwasaki, T.; Honda, K.; Furukawa, Y.; Ohdomari, I.; Kawarada, H. *Jpn. J. Appl. Phys.* **2005**, *44*, 1558−1561.

(11) Zhong, G.; Iwasaki, T.; Honda, K.; Furukawa, Y.; Ohdomari, I.; Kawarada, H. *Chem. Vap. Deposition* **2005**, *11*, 127−130.

(12) Wang, Y. Y.; Gupta, S.; Nemanich, R. *J. Appl. Phys. Lett.* **2004**, *85*, 2601−2603.

(13) Merkulov, V. I.; Melechko, A. V.; Guillorn, M. A.; Lowndes, D. H.; Simpson, M. L. *Appl. Phys. Lett.* **2001**, *79*, 2970−2972.

(14) Cheng, X.; Wang, R.; Xu, J.; Yu, D. *Micron* **2004**, *35*, 455−460.

(15) Hsu, C. H.; Lin, C. H.; Lai, H. J.; Kuo, C. T. *Thin Solid Films* **2005**, *471*, 140−144.

(16) Huang, S. *Chem. Phys. Lett.* **2003**, *374*, 157−163.

(17) Dai, H.; Rinzler, G.; Nikolaev, P.; Hess, T. A.; Colbert, T.; Smalley, R. E. *Chem. Phys. Lett.* **1996**, *260*, 471−475.

(18) Gavillet, J.; Loiseau, A.; Journet, C.; Willaime, F.; Ducastelle, F.; Charlier, J.-C. *Phys. Rev. Lett.* **2001**, *87*, 275504-1−275504-4.

(19) Bower, C.; Zhu, W.; Jin, S.; Zhou, O. *Appl. Phys. Lett.* **2000**, *77*, 830−832.

(20) Alvarez, L.; Righi, A.; Guillard, T.; Rols, S.; Anglaret, E.; Laplaze, D.; Sauvajol, J. L. *Chem. Phys. Lett.* **2000**, *316*, 186−190.

(21) Maruyama, S.; Kojima, R.; Miyauchi, Y.; Chiashi, S.; Kohno, M. *Chem. Phys. Lett.* **2002**, *10*, 229−234.

(22) Zhong, G.; Iwasaki, T.; Ohdomari, I.; Kawarada, H. To be submitted.

(23) Wang, Y.; Kim, M. J.; Shan, H.; Kittrell, C.; Fan, H.; Ericson, L. M.; Hwang, W. F.; Arepalli, S.; Hauge, R. H.; Smalley, R. E. *Nano Lett.* **2005**, *5*, 997−1002.